IFHTSE 2024: Proceedings of the 29th International Federation for
Heat Treatment and Surface Engineering World Congress
September 30–October 3, 2024, Cleveland, Ohio, USA
https://doi.org/10.31399/asm.cp.ifhtse2024p0281

Modeling Alloy Carbide Formation and Coarsening during High-temperature Tempering of Ferrium C64 Steel

Jason Meyer, and Zhichao (Charlie) Li
DANTE Solutions, Cleveland, Ohio
Jason.Meyer@dante-solutions.com

Abstract

High-alloy steels, like Ferrium C64, are used in powertrain components due to their corrosion resistance and high temperature resistance properties. These steels undergo a tempering temperature that is well above traditional steel, and during this process alloy carbides or compounds form, increasing the materials hardness, mechanical strength, and high temperature resistance properties. In the early stages of tempering, softening occurs due to the formation and coarsening of iron carbide, followed by a hardening as the alloy elements combine to form nano-scale dispersoids. These alloy carbides block the path of dislocations in the grain, strengthening the material. At longer tempering times or high temperatures, the coarsening of these alloy carbides and compounds can cause softening. A predictive material model for the high-tempering response of steels is needed to ensure peak hardening properties are met. For a robust heat treatment model, the material response for every step of the process needs to be modeled. These material properties include austenitization rates and thermal expansion during heating, carbon diffusivity and saturation limits for carburization, phase transformation rates and thermal contraction rates per phase during cooling and quenching, deep-freeze kinetics for further martensitic transformation, tempering kinetics for formation of the tempered martensite phase, and carbide kinetics for formation, coarsening, and size. Additionally, mechanical properties of each phase as a function of carbon need to be defined to ensure the proper mechanical response during and after heat treatment. After the material model is developed it can be used to design and optimize the high-temperature tempering process for any part using the same material.

Introduction

There has been a focus over the past few years to develop stronger, lighter, and high-temperature resistant materials for powertrain systems in aerospace and heavy equipment systems. From this effort, several high-alloy steels have been developed that combat the high temperature resistance with high temperature tempering. These steels include Ferrium C64, Pyrowear 675, M50NiL, and CSS-42L, which contain large amounts of alloying elements like chromium, vanadium, and molybdenum. During high temperature tempering, these compounds or carbides are on the nanometer scale and strengthen the grains by blocking paths of slip and dislocation. This leads to a higher mechanical performance and hardness when the heat treatment is done properly. If the steel is under tempered, the hardness and mechanical properties will not be met, and if over tempered the carbides will coarsen significantly reducing their hardening effectiveness. A robust materials model is needed to capture the carbide evolution during high temperature tempering to ensure optimal properties are achieved during heat treatment. Modeling this process is challenging because of the competing and dynamic mechanisms that occur during tempering. This includes carbon rejection during early stages of tempering, iron carbide formation and coarsening, and subsequent alloy carbide formation and coarsening, which are all dependent on tempering temperature, tempering time, and carbon content.

Table 1: Chemistry of select high-alloy steels.

	Ferrium C64	Pyrowear 675	M50NiL	422 SS
C	0.11%	≤0.07%	0.13%	0.2/0.25%
Mn		0.65%	0.25%	1.0%
Si		≤0.4%	0.20%	0.75%
Ni	7.5%	2.6%	3.4%	0.5/1.0%
Cr	3.5%	13.0%	4.2%	11/13%
Mo	1.75%	1.8%	4.25%	0.15/1.25%
V	0.02%	0.6%	1.2%	0.15/0.3%
Co	16.3%	5.4%		
W	0.2%			0.75/1.25%

Note: Single numbers indicate nominal value

Experimental Procedure

The typical heat treatment for high-alloy steels, like Ferrium C64, includes a normalizing step, austenitization, carburization, quenching, cryogenic treatment, and tempering at high temperatures [1]. Each step has a contribution to the final outcome, and this work focuses on the tempering step. During normalizing and austenitization steps, alloy elements diffuse and distribute relatively uniformly throughout the steel. Any existing carbides are allowed to dissolve into the solid austenite matrix, much like solution treatment in aluminum and nickel-based alloys. Carburization is often used to achieve hardness requirements on the surface of the part. Low pressure carburization (LPC) is a process often used on high alloy steel due to the more flexible control of carbide formation with the boost and diffuse steps [2]. Quenching in oil or high-pressure gas (HPGQ) is used to form martensite and lock the carbon in the martensite matrix. The deep freeze process step is important for reducing the amount of retained austenite, especially in the

case of the martensite finish temperature well below the room temperature due to the carbon and alloy composition. Figure 1 shows a comparison on hardness between an as-quenched condition and after deep freeze for carburized C64 steel. The further martensite transformation by deep freeze is clearly shown from the increase of case hardness near the surface. The hardness magnitude decreases with depth due to the carbon gradient towards the core.

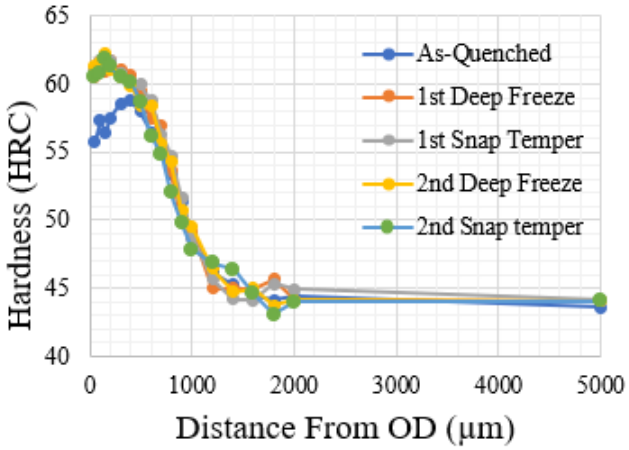

Figure 1: Hardness changes with deep freeze processing

The previous steps all contribute to the final and most important step for this work, high temperature tempering. A deep freeze step to ensure a complete martensite transformation is mandatory for C64 within 8 hours after quenching [1].

To accurately model the tempering process, an understanding of the mechanisms that occur is paramount. In the first few minutes of tempering there is a softening that occurs from the transformation of martensite to tempered martensite, and the coarsening of iron carbide. During tempering, carbon is ejected from the as-quenched martensite where it forms iron carbide. Iron carbide coarsens quickly at high temperatures, reducing their effectiveness on hardening, thus softening the steel. A "snap tempered" condition is achieved by tempering high-alloy steels at a low enough temperature that the carbon exits the matrix without effective coarsening. For this work, this snap temper condition is the starting point for the tempering study. At longer tempering times or higher temperatures, the alloying elements begin to combine with the carbon to form alloy carbides. These carbides form slower than the iron carbide, due to the slower rate of alloy element diffusion. These nano-scale carbides have an excellent hardening effect by blocking dislocation slipping. For modeling these mechanisms, a wide range of temperatures and tempering times are required to capture the iron and alloy carbide formation and coarsening rates.

The experimental sample size is 100 mm long by 10 mm diameter, machined out of 4in Ferrium C64 bar stock in the longitudinal direction. The snap tempered condition provides a starting point for the experiments, and the heat treatment process is described below:

- Austenitizing - 1000°C
- Carburization using LPC process - 1000°C
- Direct quenching using HPGQ (2 bar nitrogen)
- Double deep freeze (-101°C) and snap temper (135°C) to reduce the amount of retained austenite

A standard tempering at 500°C for 8 hours is used as the baseline to compare the results. The snap tempered samples were ready for high-temperature tempering experiments. For short time intervals, from one minute to one hour of tempering time, the samples were tempered on a Gleeble thermal-mechanical simulator. The longer tempering times were performed in a vacuum furnace at the prescribed tempering temperatures. Samples were then sectioned, and the hardness profile was used to develop material data for tempering process modeling in the DANTE heat treatment simulation software.

Results

For tempering experiments conducted at 425°C, the softening in the case is shown to occur within the first minute of tempering conducted on the Gleeble, a shown in Figure 2. During this time, the core begins to harden from alloy carbide formation. As the tempering time is increased, the hardness increases slowly as alloy carbides form uniformly throughout the sample. This tempering temperature, while lower than the suggested tempering temperature of 496°C [1], illustrates the different rates of formation and coarsening between the alloy and iron carbides. With tempering times longer than an hour at this temperature, the further hardness increase is negligible, and the obtained hardness is lower than the standard temper values. In fact, the case hardness values are lower than the snap-tempered condition due to the coarsened iron carbide and the limited hardening effect from alloy carbide formation.

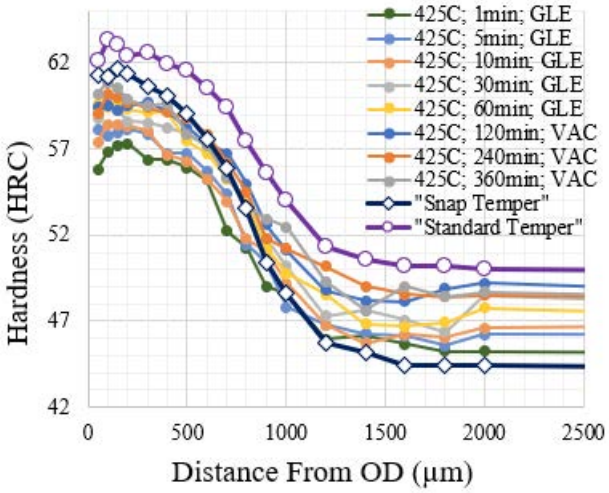

Figure 2: Hardness changes with tempering time at 425°C using Gleeble and vacuum furnace

After the first minute of tempering at 500°C, the trend of case softening and core hardening continues, as shown in Figure 3. However, the hardness in both regions is about 2 points HRC

higher than the 425°C tempering results. Here competing forces of iron carbide coarsening (softening), and alloy carbide formation (hardening) are shown. The iron carbide coarsening occurs fast and quickly reaches its valley, while the alloy carbides continue to form. After about an hour of tempering time, the hardness values reach the standard temper values, and there is no noticeable hardness change for up to 6 hours.

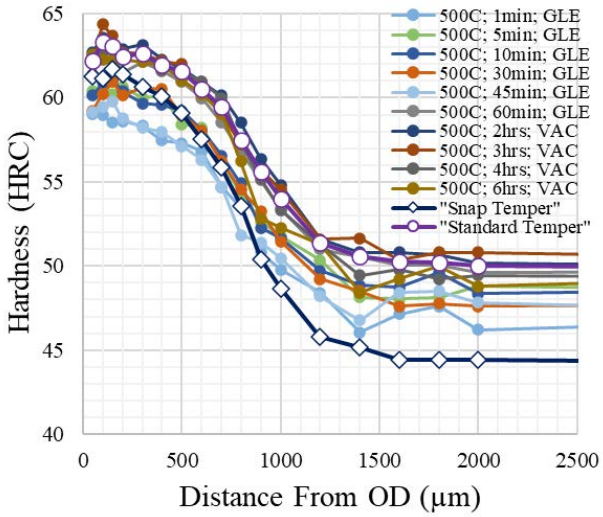

Figure 3: Hardness changes with tempering time at 500°C using Gleeble and vacuum furnace

Tempering at 575°C, the hardness in the core increases from the alloy carbide formation for the first 30 min, while the case is only slightly softer, as shown in Figure 4. Here rapid alloy carbide formation has already offset the softening from iron carbides. As tempering time continues, the effect alloy carbide coarsening on hardness drop is observed. At this temperature, the coarsening rate is high, and the hardness in the core drops below the snap temper hardness after 30 minutes of tempering. The softening of the material due to alloy carbide coarsening continues over 2 hours of tempering time.

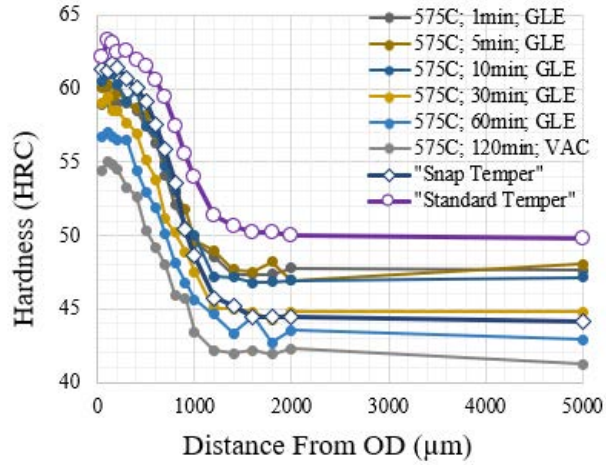

Figure 4: Hardness changes with tempering time at 575°C using Gleeble and vacuum furnace

The alloy carbides that form during heat treatment are on the nano-scale level and cannot be observed by optical microscope. To get a better understanding of the type and size of the alloy carbides, and quantify the size range, Transmission Electron Microscope (TEM) experiments were conducted. Figure 5 shows the carbide evolution during high temperature tempering for the case of the carburized cylinders.

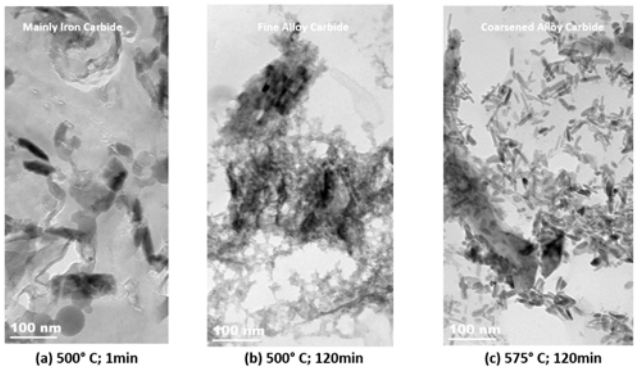

Figure 5: TEM photos showing different carbide forms of the carburized case: (a) temper at 500°C for 1 min, (b) temper at 500°C for 120 min, and (c) temper at 575°C for 120 min

After one minute of tempering time at 500°C, the carbides that exist are coarsened iron carbide, oval shaped, about 100 nm long. After 2 hours at 500°C, as shown in Figure 5(b), the alloy carbides dominate the image provided by the TEM, shown as a haze of individual carbides distributed through the microstructure. After 2 hours at 575°C, as shown in Figure 5 (c), the hazy alloy carbides have combined to form the coarsened carbides, about 30-50 nm in length. The TEM images help to validate the hardening mechanisms shown in the Gleeble experiments. The large iron carbides are not as effective at blocking deformation in the grains, thus softening the material. The nano-scale alloy carbides are very effective at blocking dislocation paths, due to their small scale and relatively uniform dispersion. When the alloy carbides are coarsened, they are less effective on hardening, illustrating the mechanism behind the secondary softening.

Modeling Development

Modeling the high temperature tempering response in high alloy steels requires several material model features to accurately describe the process. First, the decomposition of initial carbides in austenite and the completeness of the decomposition must be modeled during austenitization. The effect of carbon on the allowable amount of alloy carbide precipitation and precipitation rate has been shown to have a large effect on the rate of precipitation. If initial carbides do not dissolve effectively during austenitization, the martensite and tempered martensite phases after quenching must inherit these carbides for continuity. The volume fraction and initial size of the iron carbides will also influence the precipitation and coarsening of the alloy carbides during tempering. Both iron and alloy carbides must be modeled in the tempered martensite phase, separately. The coarsening of iron carbide causes the initial softening of the tempered martensite phase, while alloy carbide formation provides the secondary hardening response. The coarsening of alloy carbides must be modeled to capture

the softening at higher temperatures and over time. The volume change from the coarsening of iron carbide and alloy carbide coarsening is modeled to accurately predict the distortion and residual stress states. The effect of carbide sizes and their fractions on the mechanical strength of the steel is also required. Finally, the amount of carbon in alloy carbides must be related back to the total amount of carbon in the material. With these features in mind, the high-temperature tempering model was developed and implemented in the DANTE software framework.

The coarsening models were developed with a size distribution profile model, where the distribution profile is calculated from the precipitation and coarsening of the carbides. Figure 6 shows schematically the evolution of iron carbide coarsening during tempering, where the X-axis is the size class, Y-axis is the volume fraction of carbides at each size class, and the lines show the progression of tempering time.

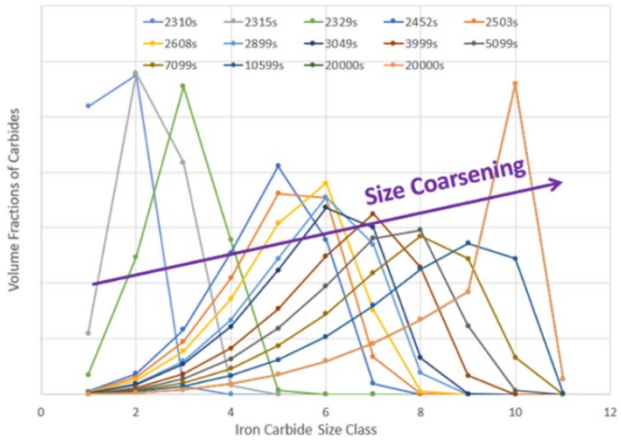

Figure 6: Simulated evolution of iron carbon size distribution during tempering.

Ten size classes are used to describe the size distribution profile, with size class 1 being the smallest carbide size and size class 10 being the largest. Size class 11 is used to represent the extreme carbide size, and is associated with very large, networked, or grain boundary carbides. As carbides form, they have an initial size of the size class 1. As tempering time increases, size class 1 gives way to size class 2 due to coarsening, and so on. The size classes also relate back to the actual size of the alloy carbides, in nanometers, defined in the DANTE material database, with definitions for size class 1 and size class 10 and the actual size distributed evenly between the size classes. Lastly, the size classes are used to determine the hardening effect of the carbides. With size class 1 contributing the most to overall hardness and size class 10 contributing the least. The size distribution and volume fraction of alloy and iron carbide profiles are converted to carbide factors, which are used to calculate the hardness and mechanical strength of the tempered martensite phase. The carbide factor is a modeling term to represent the hardening effect the carbides have on hardness and strength, with iron carbide in the snap tempered condition having the highest value. Figure 7 shows the simulated hardness evolution during tempering at various temperatures combining the iron carbide coarsening and alloy carbide precipitation and coarsening models.

The material is in the snap tempered condition initially with a hardness of about 64 HRC. The hardness quickly drops down to about 55 HRC due to the iron carbide coarsening at temperatures above 500°C, showing that the rate of softening is slower for the lower tempering temperatures, and a higher rate at elevated temperatures, as shown in Figure 7(b). After the initial softening, alloy carbides begin to form, hardening the material again, and illustrating the temperature dependence on the rate of formation and coarsening of the alloy carbides. At high temperatures, the material reaches peak hardness very quickly, but the magnitude of hardness is reduced by the alloy carbide coarsening, not even reaching the initial hardness values. Temperatures between 475°C and 525°C show hardness values that exceed the initial hardness. However, at 525°C the hardness values quickly drop below the initial hardness from the alloy carbide coarsening, while at 475°C the hardness takes a longer time, about 8 hours, to reach the initial hardness. At temperatures below 475°C, the alloy carbide formation rate is very low, and at these temperatures, the hardness never reaches the initial hardness.

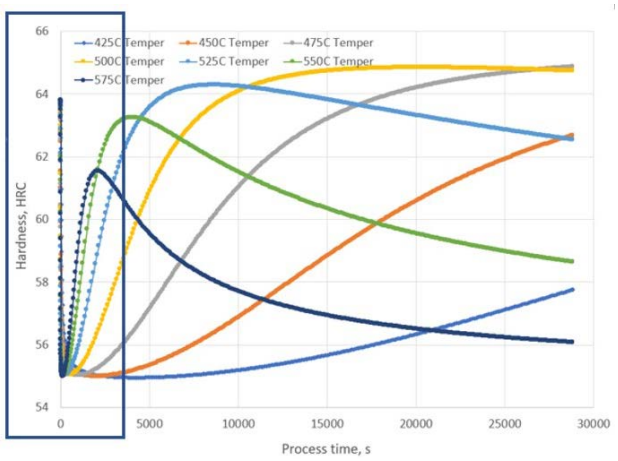

(a)

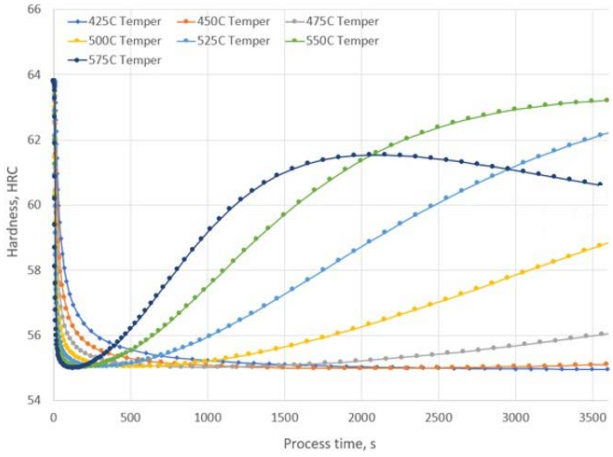

(b)

Figure 7: Simulated hardness evolution during tempering at various temperatures. (a) Plot from 0 to 3600 seconds, and (b) plot from 0 to 28800 seconds

To validate the developed models, Finite Element Analysis (FEA) models were developed using a simplified disc geometry of the bars used in the Gleeble experiments (10 mm diameter).

The full heat treatment process was modeled including low pressure carburization, 2-bar high-pressure gas quenching, double deep freeze, snap tempering, and high-temperature tempering. Figure 8 shows the cross-sectional results of two of the models, one tempered at 500°C (a) and one at 575°C (b). These results agree with the experimental results and help prove the effectiveness of the implemented tempering models.

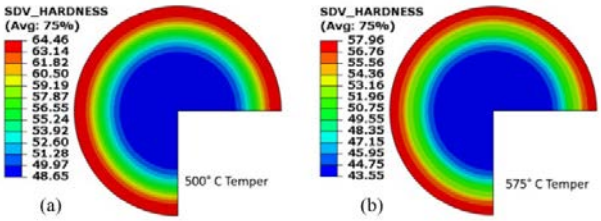

Figure 82: Predicted hardness after tempering for 3 hours at (a) 500°C and (b) 575°C

Carbon has arguably the largest effect on the hardenability of steel among the common alloy elements. An effective heat treatment model must account for the differences in carbon for the case and core. Figure 9 shows a line plot of a surface point on the cylinder model, with the blue line showing temperature and the orange line showing room-temperature hardness.

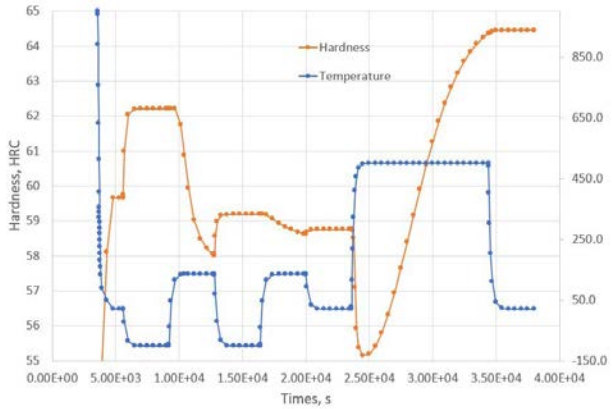

Figure 9: Hardness evolution at the surface of the carburized cylinder model during heat treatment with (a) tempering at 500°C and (b) tempering at 575°C

Initially, the hardness is very low as the phase is completely austenite. The hardness is calculated as the equivalent hardness at room temperature instead of hot hardness. The hardness increases during quenching when the austenite transforms to martensite. During the first deep freeze step, the hardness increases further as more austenite transforms to as-quenched martensite. During the first snap tempering step the hardness drops from its as-quenched values showing the conversion of as-quenched martensite to the tempered martensite phase. The second deep freeze step shows some hardening from the remaining austenite to martensite conversion and only a slight change in hardness during the second snap-temper as the remaining as-quenched martensite is converted to tempered martensite. During tempering at 500°C, the hardness drops swiftly due to the coarsening of the iron carbide, then hardens to its peak values at the end of the tempering step due to the precipitation of alloy carbide and minimum coarsening. Tempering at 575°C, the hardness also drops swiftly from iron carbide coarsening, but the peak hardness occurs much earlier, and the hardness drops due to alloy carbide coarsening.

For the base carbon range, 0.1%C, the hardness magnitudes are reduced compared to the surface values. Figure 10 shows the hardness evolution in the core of the cylinders, using the same heat treatment as Figure 9. The overall change in hardness during the deep freeze and tempering steps is small in the core where the lower carbon values reduce the effect of iron carbide coarsening on hardness. The secondary hardening occurs much faster in the core, base carbon, model reaching the peak hardness in the first few minutes of high-temperature tempering, showing the carbon concentration as the limiting factor. After the peak hardness is reached, the alloy carbide coarsening dominates until the end of the tempering step.

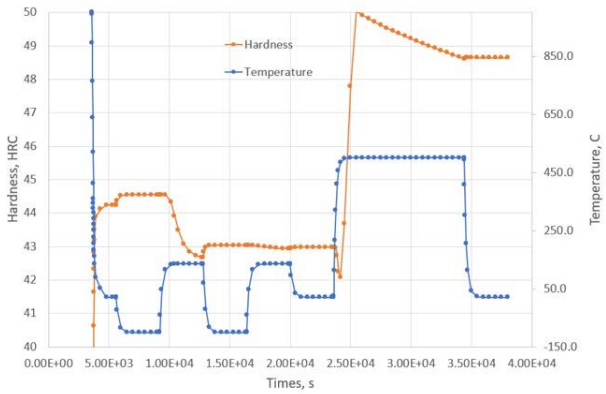

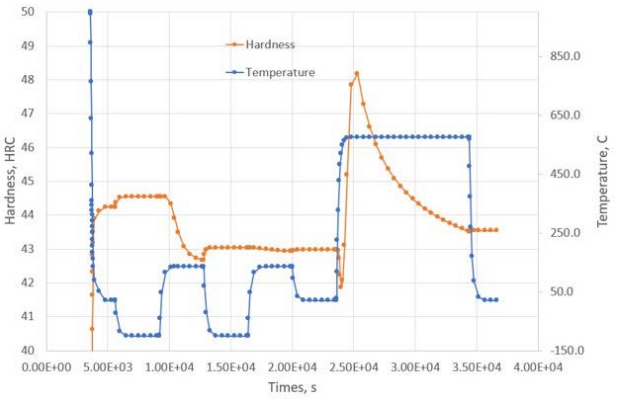

(b)

Figure 103: Hardness evolution at the core (0.1% carbon) during heat treatment with (a) tempering at 500°C and (b) tempering at 575°C

Figure 11 shows the predicted hardness profiles compared to the collected experimental data for tempering at 500°C. The predicted hardness in the snap temper condition agrees well with the experimental data shown with the orange line. After the first few minutes of tempering the DANTE model effectively captures the softening in the case from the iron carbide coarsening, beige line, with the core values slightly lower than experiments. After 3 hours of tempering the predicted hardness increases, agreeing well with the collected hardness values validating the effectiveness of the implemented carbide formation and coarsening models.

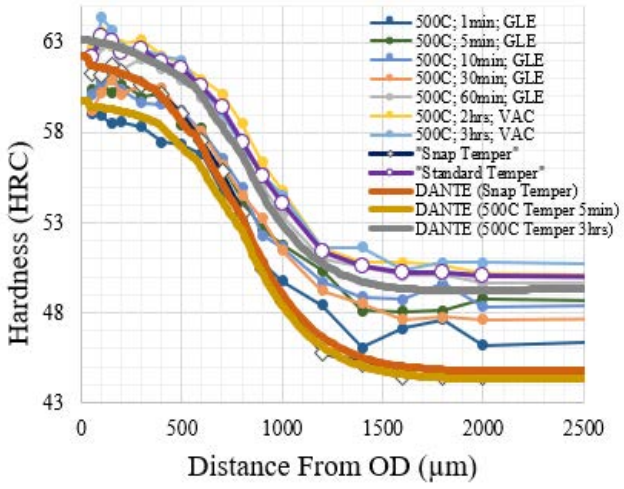

Figure 11: Predicted hardness change through the carburized case at 500°C tempering temperature

To accurately predict the distortion and residual stress after high-temperature tempering, the volume change from iron and alloy carbide coarsening must be included in the tempered martensite phase. The material volume shrinkage from iron carbide coarsening has been shown to occur within the first few minutes of tempering, which is one of the primary mechanisms of distortion and residual stress change during tempering. The precipitation of alloy carbides can expand or shrink the volume of the tempered martensite, and this effect is often dependent on alloy composition. The coarsening of alloy carbides is expected to have a volume shrinkage with a magnitude less than the iron carbide coarsening. Figure 12 shows a simulated dilatometry curve showing the difference in volume using the developed iron carbide coarsening model and alloy carbide precipitation and coarsening models.

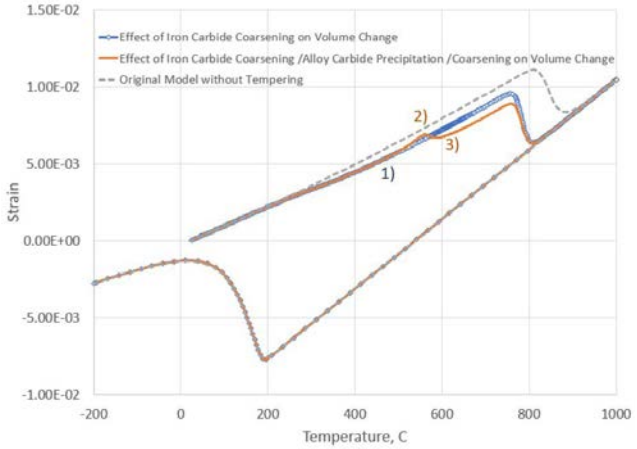

Figure 12: Volume change of tempered martensite due to various possible mechanisms

Starting with the martensite phase at room temperature the grey line shows an austenitization and quench model without tempering of the obtained martensite. The blue line shows tempering effect including the iron carbide coarsening, with the volume shrinkage occurring after 300°C during heat up, (1). The orange line shows the developed alloy carbide formation (2) and coarsening (3) models.

While the alloy carbide effect is very slight, the accuracy of the model is improved by accounting for these volume effects, especially for distortion and residual stress. The residual compressive stress in the samples processed at 500°C was shown to have a significant decrease in magnitude, from about -400MPa to about -200 MPa, from the snap tempered to high-temperature tempered conditions, as shown in Figure 13. This reduction in compressive stress is mainly caused by the more volume shrinkage in the case than the core due to the iron carbide coarsening. The formation and coarsening of alloy carbides during high temperature tempering at 500°C shows very little effect on the residual stress over the 6-hour tempering time, overshadowed by the scatter of data. The DANTE model prediction for the simplified cylinder model agrees with the collected data, with the initial snap tempered condition more compressive in the case than the high temperature tempering model.

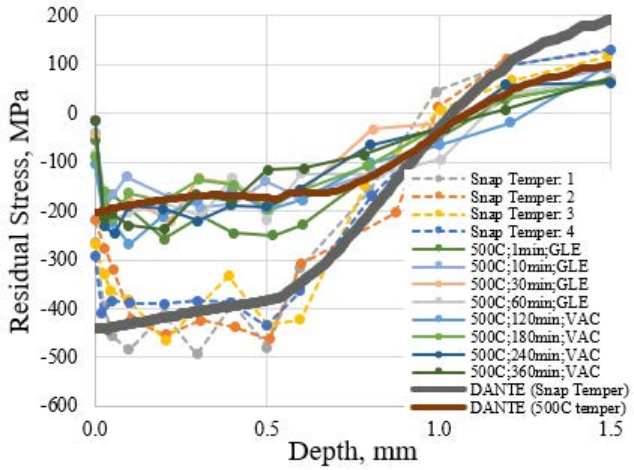

Figure 13: Predicted axial residual stress in the carburized cylinder, compared to experimental results

Conclusions

High alloy steels that undergo a high-temperature tempering process show an initial softening from iron carbide coarsening, then a hardening from alloy carbide formation. Depending on the tempering temperature and tempering time, the alloy carbides can then coarsen, which causes material softening. Experiments were conducted over a wide range of tempering times and temperatures on samples made from Ferrium C64 steel to quantify the carbide formation and coarsening that occurs early in the tempering process. DANTE heat treatments models were developed to predict the hardness response from high temperature tempering in order to simulate and optimize the process. Finite element models were used to simulate the experimental geometry and processing conditions, and the simulations can effectively capture the different rates of iron carbide coarsening and alloy carbide formation and coarsening, agreeing well with the experimental data. The material volume change from iron carbide coarsening, and alloy carbide formation and coarsening were developed, and the residual stress prediction was validated. Once developed, the models can be used to develop new processes and optimize existing processes, while ensuring material specifications are met.

References

[1] “Ferrium C64 Datasheet.” Carpenter Technologies, CRS Holdings LLC, 2022.

[2] Ferguson, B. Lynn, et al. “Vacuum carburizing steel alloys containing strong carbide formers.” Heat Treat 2017: Proceedings from the 29th Heat Treating Society Conference and Exposition, 24 Oct. 2017.